Annihilations of Antiprotons at Rest in Hydrogen. V. Multipion Annihilations*

C. BALTAY, P. FRANZINI, G. LÜTJENS,† J. C. SEVERIENS, D. TYCKO, AND D. ZANELLO‡
Columbia University, New York, New York

Approximately 45 000 pionic annihilations of stopped antiprotons in hydrogen have been measured and analyzed. The relative annihilation rates into the various multipion final states are presented. The experimental distributions of the invariant masses of all the possible pion combinations have been obtained. Strong production of the ρ, ω, and η meson has been observed, and their production rates have been established. The rates for simultaneous production of $\rho^0\rho^0$, $\rho^0\omega^0$, and $\rho^0\eta^0$ are discussed.

I. INTRODUCTION

A STUDY of the annihilation of stopped antiprotons in hydrogen into pions has been carried out. The antiprotons were produced in the Brookhaven AGS and were stopped in the 30-in. Columbia-BNL hydrogen bubble chamber.[1] A total of 7127 events with two charged prongs, 36 823 events with four charged prongs, and 549 events with six charged prongs were analyzed.

A similar study, based on fewer events, has been performed by the Oxford-Padua collaboration.[2]

A general symmary of the results on pionic annihilations is presented in this paper. Some particular reactions have been analyzed and the results are presented in Refs. 3 to 8.

II. EXPERIMENTAL METHOD

The photographs of the 30-in. chamber used for this study contained an average number of 1.5 antiproton stops per picture. A small, cylindrical fiducial volume of 20 cm radius and 20 cm depth was used, to improve the resolution of the measurements. Only one-seventh of the stopping antiprotons were in this reduced volume. The film was scanned and measured in one operation.

For a part of the film annihilations into zero charged prongs were recorded. Events where one of the charged tracks could be identified as a K meson, and events with associated K^0 decays, were not measured. Events with n charged prongs plus an obvious Dalitz pair were measured as n prongs, ignoring the Dalitz pair. (Obvious Dalitz pairs were defined as two lightly ionizing tracks, with less than a 3° angle between them, and with at least one of the tracks going around half a circle or more in the chamber without stopping.) No further corrections for Dalitz pairs were made in the annihilation rates. Portions of the film were scanned twice; it could be concluded from the comparison of the two scans that the scanning efficiencies for two, four and six-pronged annihilations were the same, approximately 85% for a single scan.

About one-third of the measurements were performed on high-precision film-plane digitizers, and two thirds were performed on image-plane digitizers. The resolution of the two kinds of machines was sufficiently similar in the present experiment for the measurements from the two to be combined. The measurements were processed by a geometrical reconstruction program,[9] NP54, and a version of the CERN GRIND[10] kinematics program. In cases where one of the charged prongs scattered in the hydrogen, the scattering products were also measured. This information was used in the kinematic fitting programs, so that any biases in the results due to the different scattering cross sections of π^+ and π^- in hydrogen were reduced to a negligible amount. All charged prongs were assumed to be pions; kinematic fits were tried for each event corresponding to 0 or 1 missing neutral pion. Events were classified as having 0, 1 or more than 1 missing neutral pion by using the χ^2 values obtained in the kinematic fits and the missing mass at the annihilation vertex, computed from the measured quantities, by the following criteria:

(a) Events were classified as 0 missing π^0's if the corresponding fit had $\chi^2 \leq 6$ times the number of constraints.

(b) Events were classified as 1 missing π^0 if the 4 constraint fit to no missing π^0's was unacceptable and

* Work supported in part by the U. S. Atomic Energy Commission.

† Present address: Max-Planck Institut für Physik, Munchen, Germany.

‡ NATO Fellow, 1964–1965.

[1] For the design and performance of the low-energy separated beam, see D. Berley, AGS Internal Report DB-1, 1963 (unpublished) and C. Alff-Steinberger, Ph.D. thesis submitted to Columbia University, 1964 (Nevis Report No. 126) (unpublished).

[2] M. Cresti, A. Grigoletto, S. Limentani, A. Loria, L. Peruzzo, R. Santangelo, G. B. Chadwick, W. T. Davies, M. Derrick, C. J. B. Hawkins, P. M. B. Gray, J. H. Mulvey, P. B. Jones, D. Radojicic, and C. A. Wilkinson, in *Proceedings of the Siena International Conference on Elementary Particles and High Energy Physics, 1963*, edited by G. Bernadini and G. P. Puppi (Societá Italiana di Fisica, Bologna, 1963), p. 263.

[3] N. Barash, P. Franzini, L. Kirsch, D. Miller, J. Steinberger, T. H. Tan, R. Plano, and P. Yeager, Phys. Rev. **139**, B1659 (1965).

[4] C. Baltay, P. Franzini, N. Gelfand, G. Lütjens, J. C. Severiens, J. Steinberger, D. Tycko, and D. Zanello, Phys. Rev. **140**, B1039 (1965).

[5] C. Baltay, P. Franzini, G. Lütjens, J. S. Severiens, J. Steinberger, D. Tycko, and D. Zanello, Phys. Rev. **140**, B1042 (1965).

[6] N. Barash *et al.*, preceding paper, **144**, 1095 (1966).

[7] C. Baltay, N. Barash, P. Franzini, N. Gelfand, L. Kirsch, G. Lütjens, D. Miller, J. C. Severiens, J. Steinberger, T. H. Tan, D. Tycko, D. Zanello, R. Goldberg, and R. J. Plano, Phys. Rev. Letters **15**, 532 597(E) (1965).

[8] C. Baltay, N. Barash, P. Franzini, N. Gelfand, L. Kirsch, G. Lütjens, D. Miller, J. C. Severiens, J. Steinberger, T. H. Tan, D. Tycko, D. Zanello, R. Goldberg, and R. J. Plano, Phys. Rev. Letters **15**, 591 (1965).

[9] R. J. Plano and D. H. Tycko, Nucl. Instr. Methods **20**, 458 (1963).

[10] R. Böck, CERN Report 61-29, 1961 (unpublished).

TABLE I. Annihilation rates for multipion production.

Reaction	No. of events in fid. vol.	Corrected No. of events	Annihilation rate (%)
$\bar{p}p \rightarrow$ total 0 prongs	157		3.2 ±0.5
$\bar{p}p \rightarrow \pi^+\pi^-$	78	78	0.32±0.03[a]
$\pi^+\pi^-\pi^0$	823	1210	7.8 ±0.9
$\pi^+\pi^- x^0$	6226	5839	34.5 ±1.2
total 2 prongs	7127	7127	42.6 ±1.1
$\bar{p}p \rightarrow \pi^+\pi^+\pi^-\pi^-$	4621	4621	5.8 ±0.3
$\pi^+\pi^+\pi^-\pi^-\pi^0$	13 793	15 033	18.7 ±0.9
$\pi^+\pi^+\pi^-\pi^- x^0$	18 409	17 169	21.3 ±1.1
total 4 prongs	36 823	36 823	45.8 ±1.0
$\bar{p}p \rightarrow \pi^+\pi^+\pi^+\pi^-\pi^-\pi^-$	279	279	1.9 ±0.2
$\pi^+\pi^+\pi^+\pi^-\pi^-\pi^-\pi^0$	217	236	1.6 ±0.3
$\pi^+\pi^+\pi^+\pi^-\pi^-\pi^- x^0$	53	34	0.3 ±0.1
total 6 prongs	549	549	3.8 ±0.2
Total pionic annihilations			95.4 ±1.6

[a] The rate (0.32±0.03)% is not based on the 78 events observed in the present study. It is based on a previous extensive search for collinear two-pronged events in the same stopping antiproton exposure [C. Baltay *et al.*, phys. Rev. Letters **15**, 532, 597(E) (1965)].

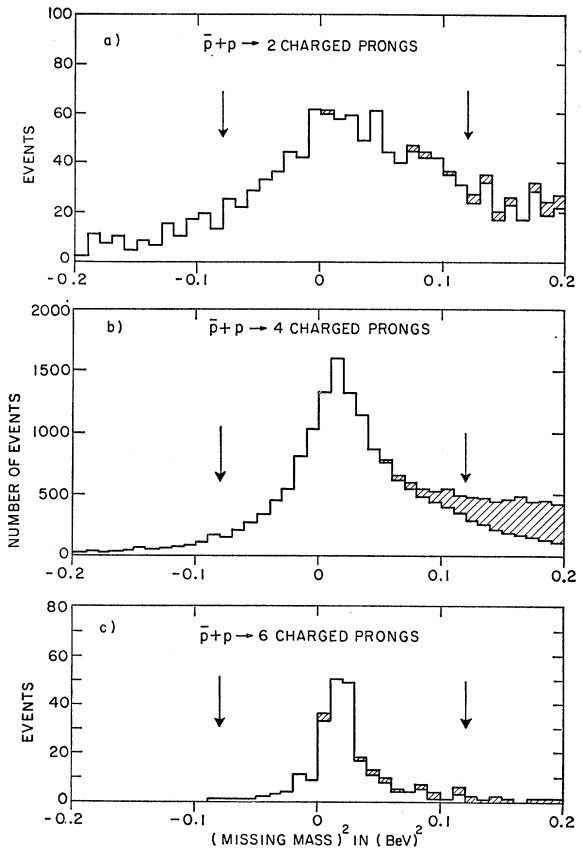

FIG. 1. Distributions in the square of the missing mass for the annihilations at rest into (a) 2 charged prongs, (b) 4 charged prongs, and (c) 6 charged prongs. The shaded areas represent events which did not achieve a kinematic fit ($\chi^2>6$) to a single missing π^0 hypothesis. The arrows indicate the cutoffs in the square of the missing mass used in classifying events as one or more than one missing π^0 events.

the 1-constraint fit had $\chi^2\leq 6$, and the square of the missing mass was within 0.1 BeV^2 of the square of the π^0 mass.

(c) Events were classified as more than 1 missing π^0 if the fit to no π^0's was unacceptable, and the fit to 1 missing π^0 had $\chi^2>6$, or the square of the missing mass was larger than the square of the π^0 mass by more than 0.1 BeV^2.

III. ANNIHILATION RATES

In approximately one third of the film used in this experiment all annihilations with 0, 2, 4, and 6 charged prongs were counted. This count was used to determine the annihilation rates as a function of the charged

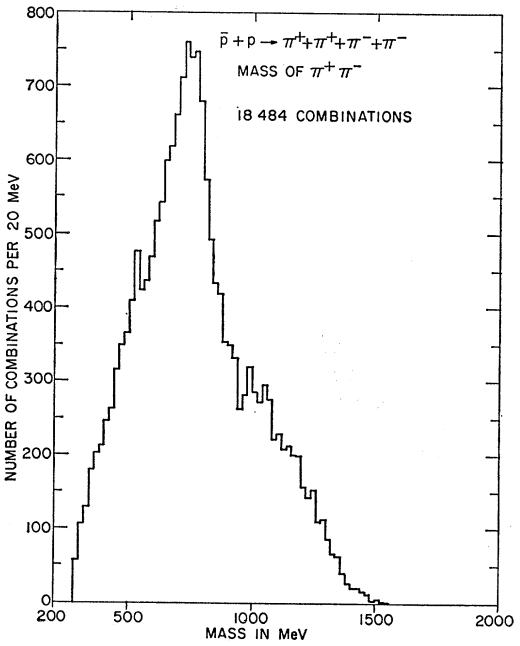

FIG. 2. Distribution in the invariant mass of $\pi^+\pi^-$ in the reaction $\bar{p}+p \rightarrow \pi^+ + \pi^+ + \pi^- + \pi^-$.

pion multiplicity. In this count events with obvious $K^\pm$ or associated K^0's were included; to get the pure pionic rates, the known annihilation rates into kaons[11] were subtracted. The count yielded 593, 7324, 7527, and 615 annihilations with 0, 2, 4, and 6 charged prongs, respectively. After subtracting the annihilations into kaons, the rates for pionic annihilations with 0, 2, 4, and 6 charged prongs were found to be (3.2±0.5)%, (42.6±1.1)%, (45.8+1.0)% and (3.8±0.2)%, respectively.

To obtain the rates for annihilations with zero, one, or more than one π^0 in each charged-prong category, the assumption was made that the losses in the geometry and kinematic programs were independent of the num-

[11] N. Barash and L. Kirsch (private communication).

ber of π^0's. This assumption was necessary since events rejected by these programs were not remeasured.[12]

The number of events which satisfied the selection criteria stated in Sec. II are shown in the first column of Table I for the various pionic channels. Events with no π^0's were identified by four-constraint kinematic fits and no further correction to their numbers were necessary. Events with a single π^0, however, were selected on the basis of a cutoff in the missing-mass spectra; their numbers had to be corrected for true single π^0 events falling outside the cutoffs, and for multi-π^0 events falling inside the cutoffs. The distribution in the square of the missing mass for the 2, 4, and 6 pronged events are shown in Figs. 1(a), 1(b) and 1(c), respectively. In these figures all events have been

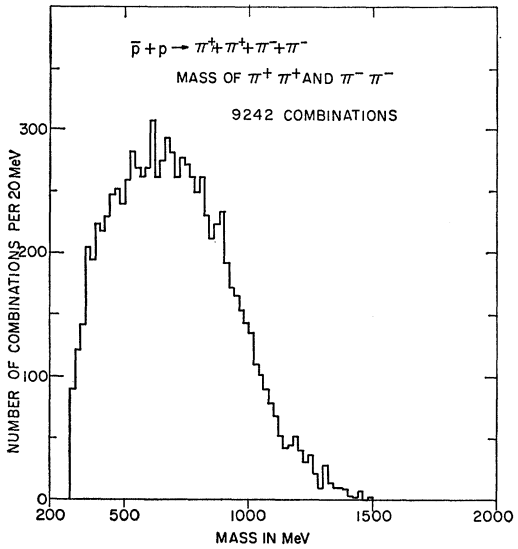

FIG. 3. Distribution in the invariant mass of $\pi^+\pi^+$ and $\pi^-\pi^-$ in the reaction $\bar{p}+p \to \pi^+ + \pi^+ + \pi^- + \pi^-$.

included except those which satisfy 4 constraint fits to no missing π^0. The shaded regions indicate events for which no satisfactory 1 constraint fits to single π^0 production were made. From a study of these distributions, the correction factors by which the number of events satisfying the criteria for single π^0 events have to be multiplied were estimated to be 1.37 ± 0.14, 1.05 ± 0.03, and 1.00 ± 0.02 for 2, 4, and 6 prongs, respectively. A further correction was made for true single π^0 events which did not make 1-constraint fits because the momentum of one of the pions was too poorly measured. The number of events thus corrected are shown in column 2 of Table I. The annihilation rates

[12] Of the total number of events measured, 5.6% were rejected by the geometrical reconstruction programs; these rejects are independent of the number of π^0's produced in any given charged prong category. Of the events measured 4.5% were rejected by the kinematical fitting programs; of these 2.1%, 2.2% and 0.2% were events with 2, 4, and 6 charged prongs, respectively. The uncertainty in the division of these rejects between zero, one, or more than one π^0 events is within the errors on the rates for these channels quoted in Table I.

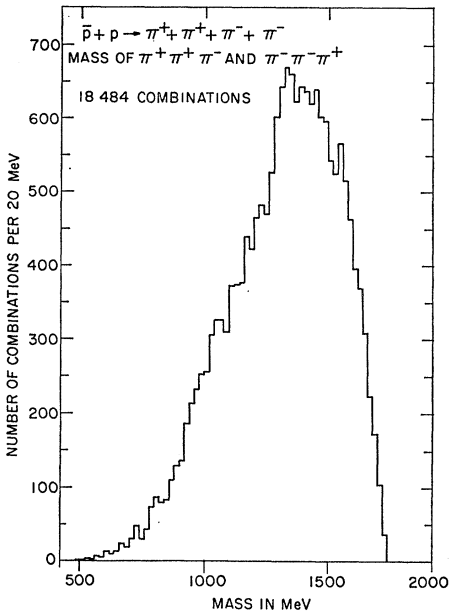

FIG. 4. Distribution in the invariant mass of $\pi^+\pi^+\pi^-$ and $\pi^-\pi^-\pi^+$ in the reaction $\bar{p}+p \to \pi^+ + \pi^+ + \pi^- + \pi^-$.

(the number of annihilations of a certain type divided by the total number of $\bar{p}$ stops[13]) are shown in column 3 of Table I.

IV. INVARIANT-MASS DISTRIBUTIONS

The Dalitz plot and its projections for the annihilation into three pions have been published.[4] The invariant mass distributions for all the possible combinations of pions are shown in Figs. 2 to 21 for the events with

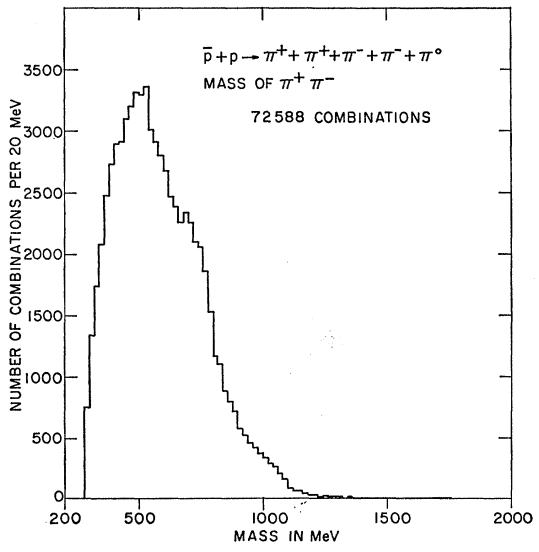

FIG. 5. Distribution in the invariant mass of $\pi^+\pi^-$ in the reaction $\bar{p}+p \to \pi^+ + \pi^+ + \pi^- + \pi^- + \pi^0$.

[13] No corrections were made for the fact that some small fraction of the annihilations were actually due to antiprotons in flight. For the pionic annihilations, these corrections were estimated to be within the quoted errors on the annihilation rates.

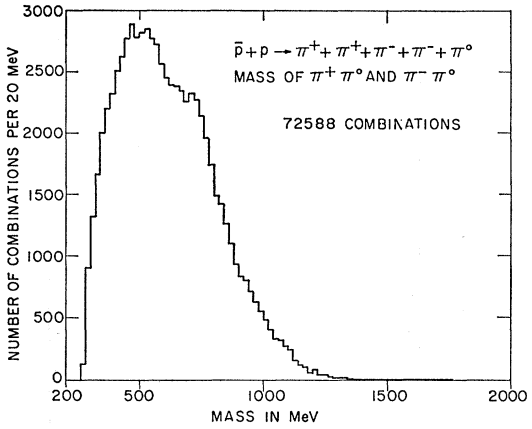

FIG. 6. Distribution in the invariant mass of $\pi^+\pi^0$ and $\pi^-\pi^0$ in the reaction $\bar{p}+p \to \pi^+ + \pi^+ + \pi^- + \pi^- + \pi^0$.

4 charged pions. Since no violation of charge conjugation invariance is apparent in $\bar{p}p$ annihilations at rest,[8] all the charge conjugate distributions were combined.

The multi-π^0 contamination in the 2-pronged events which were classified as single π^0 events was estimated by putting all 4-pronged events through the kinematics programs using the measurements of two of the charged prongs only. Only $\frac{3}{4}\%$ of all 4-pronged events satisfied the criteria for $\pi^+\pi^-\pi^0$ events. The number of 2-pronged events with more than one missing π^0 is roughly five times the number of $\pi^+\pi^-\pi^0$ events; $\frac{3}{4}\%$ of these events, which we take to be the multi-π^0 contamination in the $\pi^+\pi^-\pi^0$ events, amounts to $\sim 4\%$ of the $\pi^+\pi^-\pi^0$ events. The corresponding estimate for the multi-π^0 contamination in the $\pi^+\pi^+\pi^-\pi^-\pi^0$ events was not done because of the small number of events with 6 charged prongs. An upper limit of 10% can be put on this contamination from the distribution in the square of the missing mass in the 4-pronged events [Fig. 1(b)], using the assumption that this distribution for the single π^0 events is symmetric about the square of the π^0 mass.

The distributions for events with more than one missing π^0 do not include events which satisfy the 1 constraint fit to a single missing π^0 even if the missing mass for the event is outside the cutoff used for single π^0 events; there should be thus negligible single π^0 contamination in these events.

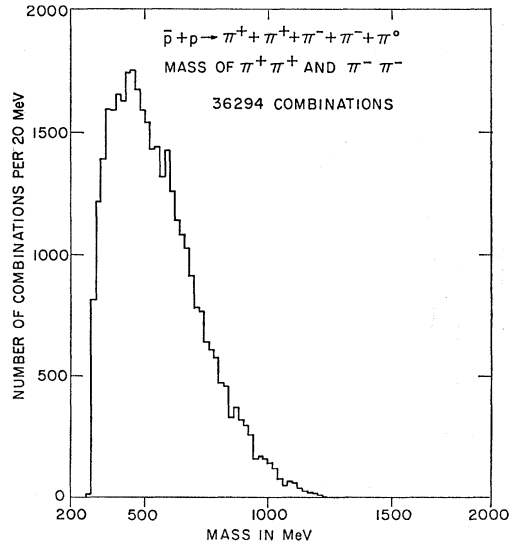

FIG. 7. Distribution in the invariant mass of $\pi^+\pi^+$ and $\pi^-\pi^-$ in the reaction $\bar{p}+p \to \pi^+ + \pi^+ + \pi^- + \pi^- + \pi^0$.

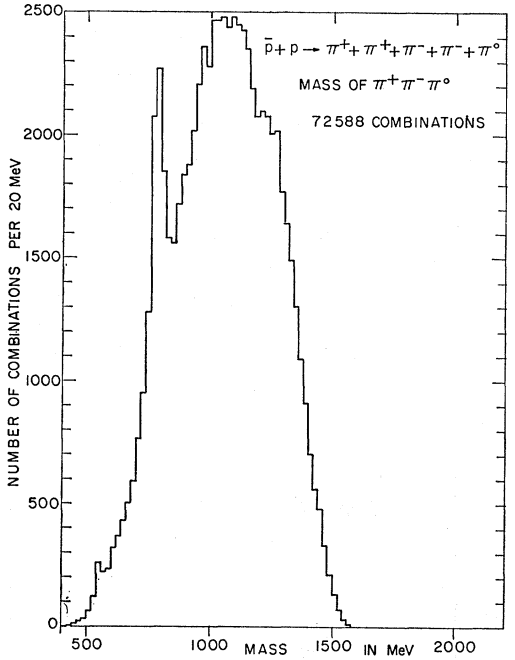

FIG. 8. Distribution in the invariant mass of $\pi^+\pi^-\pi^0$ in the reaction $\bar{p}+p \to \pi^+ + \pi^+ + \pi^- + \pi^- + \pi^0$.

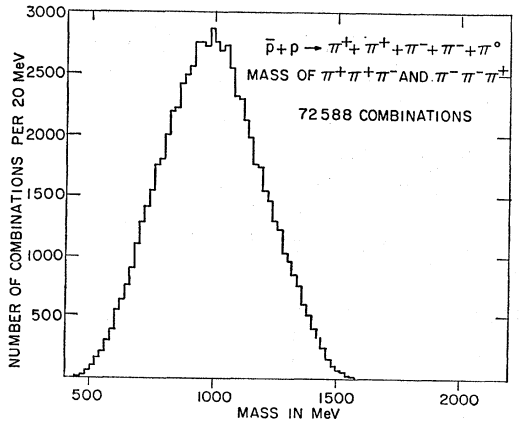

FIG. 9. Distribution in the invariant mass of $\pi^+\pi^+\pi^-$ and $\pi^-\pi^-\pi^+$ in the reaction $\bar{p}+p \to \pi^+ + \pi^+ + \pi^- + \pi^- + \pi^0$.

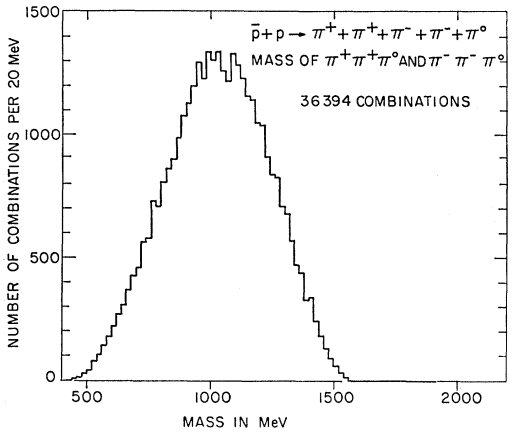

FIG. 10. Distribution in the invariant mass of $\pi^+\pi^+\pi^0$ and $\pi^-\pi^-\pi^0$ in the reaction $\bar{p}+p \rightarrow \pi^+ + \pi^+ + \pi^- + \pi^- + \pi^0$.

V. PRODUCTION OF THE ϱ, ω, AND η RESONANCES

As has been observed previously,[2] the ρ^0, $\rho^\pm$, and ω^0 mesons are produced prominently in $\bar{p}p$ annihilations at rest (see Figs. 2, 5, 6, and 8). There is also evidence for the production of the η^0 meson. The evaluation of the production rates of these resonances is made difficult by the fact that the backgrounds cannot be adequately fitted by phase space in most of the annihilation channels of $\bar{p}p$ at rest. For a careful evaluation of these rates the proper matrix elements should be written taking into account the Bose statistics of the pions and the restrictions on the angular momentum and isospin states available from S-wave $\bar{p}p$ annihilations. This was done for the 3π and the $\omega\pi\pi$ final states,[4,5] but for four- and five-body final states this procedure becomes overly complex. The situation is further complicated by the possible existence of heavier resonant states that may decay into $\rho\pi$, $\omega\pi$, or $\eta\pi$.

A simpler method was used instead to get a rough estimate for the amount of resonance production. Only the region of the invariant mass spectrum near the resonance in question was considered, and was fitted

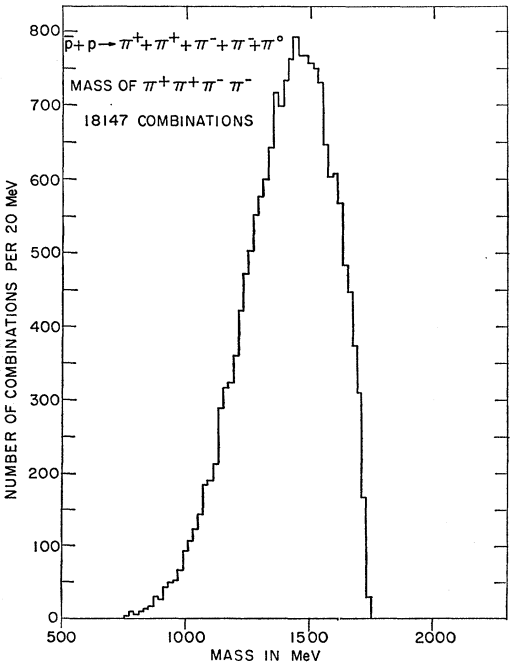

FIG. 11. Distribution in the invariant mass of $\pi^+\pi^+\pi^-\pi^-$ in the reaction $\bar{p}+p \rightarrow \pi^+ + \pi^+ + \pi^- + \pi^- + \pi^0$.

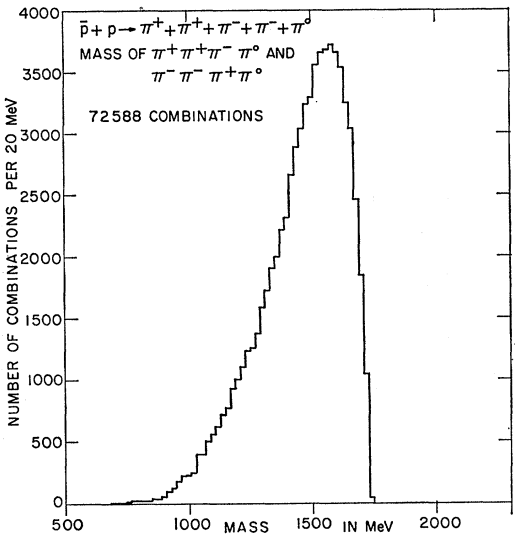

FIG. 12. Distribution in the invariant mass of $\pi^+\pi^+\pi^-\pi^0$ and $\pi^-\pi^-\pi^+\pi^0$ in the reaction $\bar{p}+p \rightarrow \pi^+ + \pi^+ + \pi^- + \pi^- + \pi^0$.

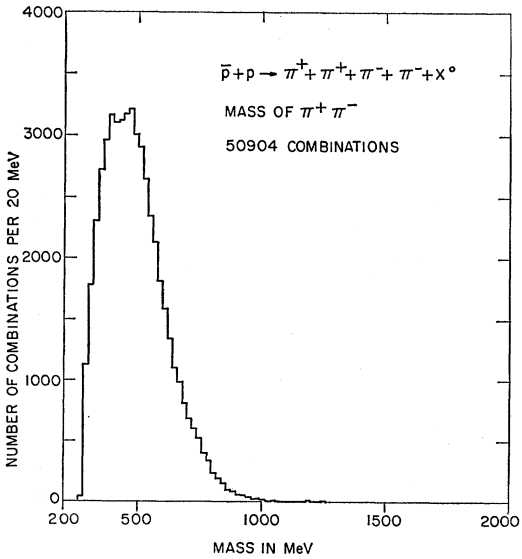

FIG. 13. Distribution in the invariant mass of $\pi^+\pi^-$ in the reaction $\bar{p}+p \rightarrow \pi^+ + \pi^+ + \pi^- + \pi^- + X^0$.

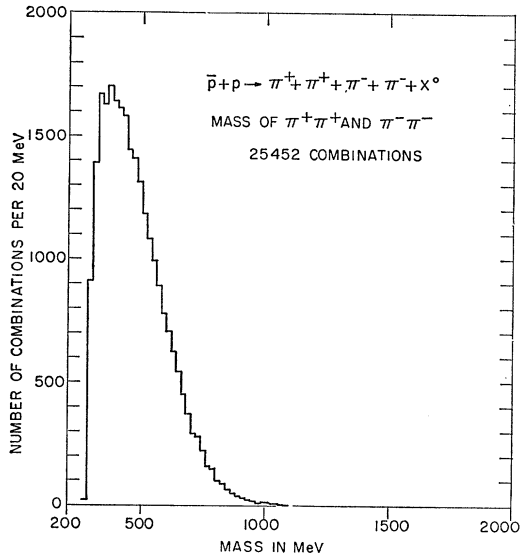

FIG. 14. Distribution in the invariant mass of $\pi^+\pi^+$ and $\pi^-\pi^-$ in the reaction $\bar{p}+p \to \pi^+ + \pi^+ + \pi^- + \pi^- + X^0$.

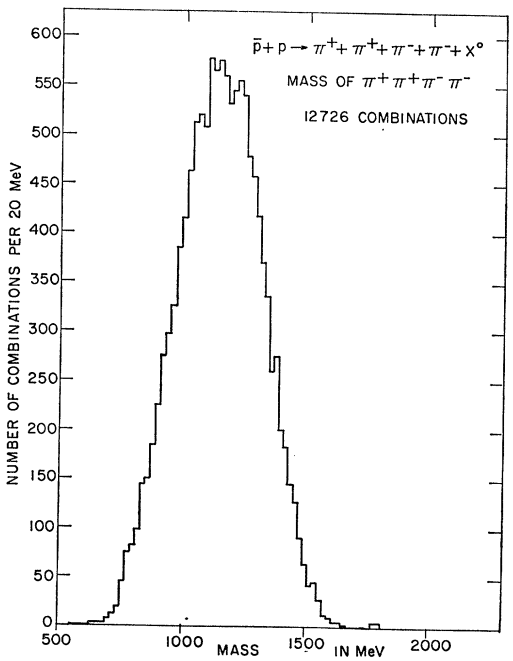

FIG. 16. Distribution in the invariant mass of $\pi^+\pi^+\pi^-\pi^-$ in the reaction $\bar{p}+p \to \pi^+ + \pi^+ + \pi^- + \pi^- + X^0$.

to a Breit-Wigner resonance shape multiplied by phase space, plus a second- or third-order polynomial for background.

A. ω^0 and η^0 Production

For a narrow resonance like the ω^0 and the η^0 this procedure is quite good. A Gaussian rather than a Breit-Wigner shape was used to fit the ω^0 and the η^0 since the width due to resolution is larger in the present case than the natural width of the states. The fits were done to the $\pi^+\pi^-\pi^0$ invariant mass distribution in the reaction $\bar{p}+p \to \pi^+ + \pi^+ + \pi^- + \pi^- + \pi^0$. The region used for the η^0 was $450 \leq M_{3\pi} \leq 650$ MeV, and for the ω^0 was $700 \leq M_{3\pi} \leq 900$ MeV. Both were adequately fitted by a Gaussian (centered at 780.5 MeV with $\sigma \approx 19$ MeV for the ω^0 and 548 MeV with $\sigma \approx 15$ MeV for the η^0) and a second order polynomial. The fits are shown in Figs. 22 and 23.

The area of the Gaussian corresponded to (17.5 $\pm$1.3)% of the $\pi^+\pi^+\pi^-\pi^-\pi^0$ events in the case of the ω^0.

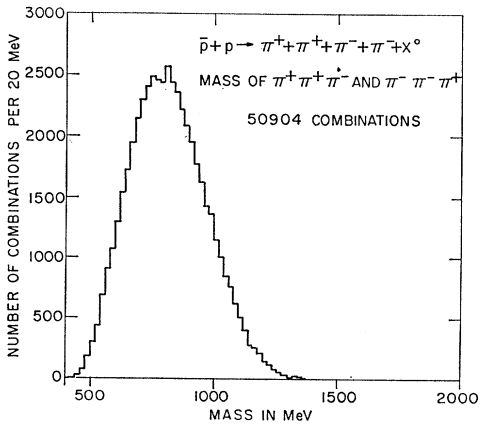

FIG. 15. Distribution in the invariant mass of $\pi^+\pi^+\pi^-$ and $\pi^-\pi^-\pi^+$ in the reaction $\bar{p}+p \to \pi^+ + \pi^+ + \pi^- + \pi^- + X^0$.

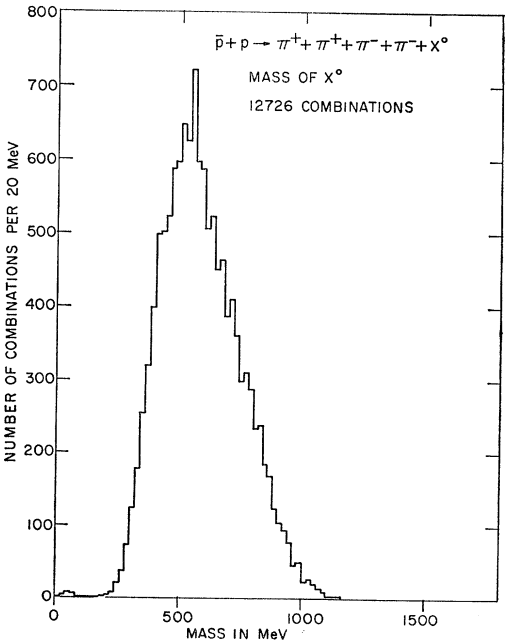

FIG. 17. Distribution in the invariant mass of X^0 in the reaction $\bar{p}+p \to \pi^+ + \pi^+ + \pi^- + \pi^- + X^0$.

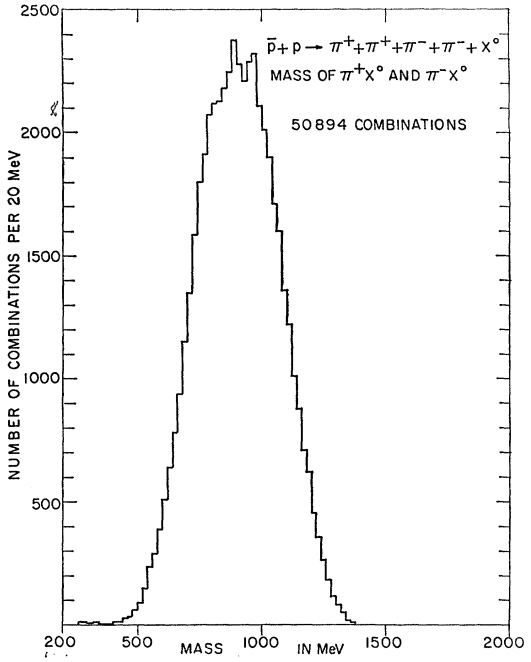

FIG. 18. Distribution in the invariant mass of π^+X^0 and π^-X^0 in the reaction $\bar{p}+p \rightarrow \pi^+ + \pi^+ + \pi^- + \pi^- + X^0$.

Using the ratio 1.14 for $(\omega^0 \rightarrow \text{all})/(\omega^0 \rightarrow \pi^+\pi^-\pi^0)$, the rate for $\bar{p}p \rightarrow \omega^0 + \pi^+ + \pi^-$ is $(3.8 \pm 0.4)\%$.

In the case of the η^0 the area of the Gaussian corresponded to $(1.84 \pm 0.2)\%$ of all $\pi^+\pi^+\pi^-\pi^-\pi^0$ events; using 3.5 for the ratio $(\eta^0 \rightarrow \text{all})/(\eta^0 \rightarrow \pi^+\pi^-\pi^0)$, the absolute annihilation rate for $\bar{p}p \rightarrow \eta^0\pi^+\pi^-$ is $(1.2 \pm 0.3)\%$.

B. ρ Meson Production

The present procedure used to evaluate the resonance production rates is less accurate for the ρ meson because

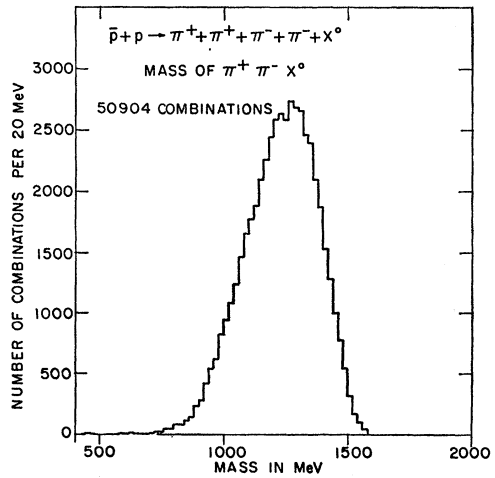

FIG. 19. Distribution in the invariant mass of $\pi^+\pi^-X^0$ in the reaction $\bar{p}+p \rightarrow \pi^+ + \pi^+ + \pi^- + \pi^- + X^0$.

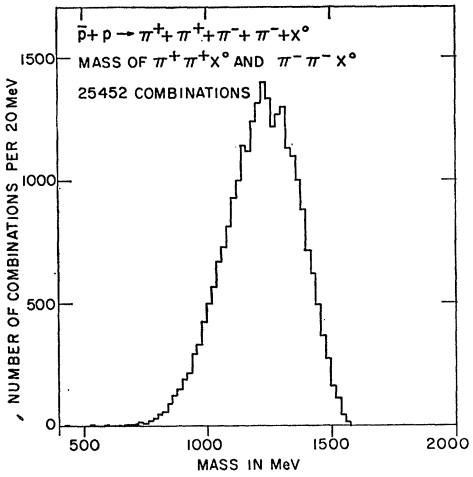

FIG. 20. Distribution in the invariant mass of $\pi^+\pi^+X^0$ and $\pi^-\pi^-X$ in the reaction $\bar{p}+p \rightarrow \pi^+ + \pi^+ + \pi^- + \pi^- + X^0$.

of its larger width. This is reflected in the larger errors on the ρ production rates. Three mass spectra were used, with each event contributing four combinations:

$$\text{mass of } \pi^+\pi^- \text{ in } \bar{p}p \rightarrow \pi^+\pi^+\pi^-\pi^-,$$
$$\text{mass of } \pi^+\pi^- \text{ in } \bar{p}p \rightarrow \pi^+\pi^+\pi^-\pi^-\pi^0,$$
$$\text{mass of } \pi^\pm\pi^0 \text{ in } \bar{p}p \rightarrow \pi^+\pi^+\pi^-\pi^-\pi^0.$$

The mass and width of the ρ were left free parameters in these fits. The mass region $400 \leq M_{2\pi} \leq 980$ MeV was used for the 4π events and $560 \leq M_{2\pi} \leq 960$ MeV for the 5π events. The parameters of the best fits obtained are given in Table II. The fraction of resonance production was taken to be the number of events corresponding

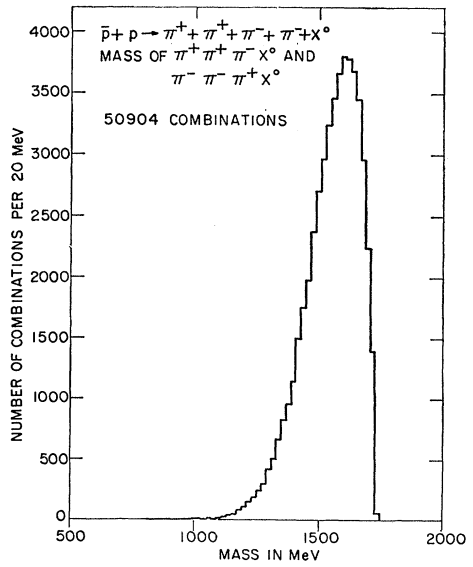

FIG. 21. Distribution in the invariant mass of $\pi^+\pi^+\pi^-X^0$ and $\pi^-\pi^-\pi^+X^0$ in the reaction $\bar{p}+p \rightarrow \pi^+ + \pi^+ + \pi^- + \pi^- + X^0$.

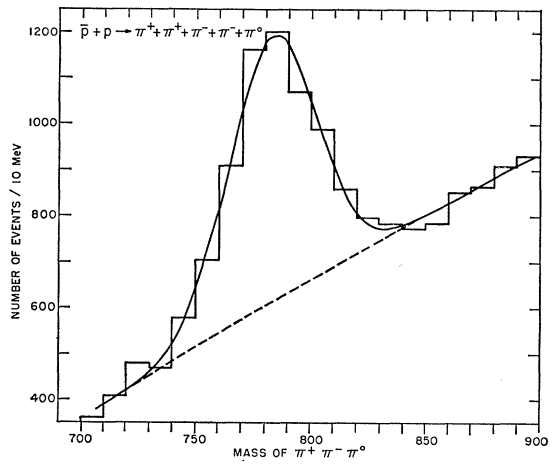

FIG. 22. Fit to the $\pi^+\pi^-\pi^0$ mass spectrum near the ω^0 region in $\bar{p}+p \to \pi^+ + \pi^+ + \pi^- + \pi^- + \pi^0$.

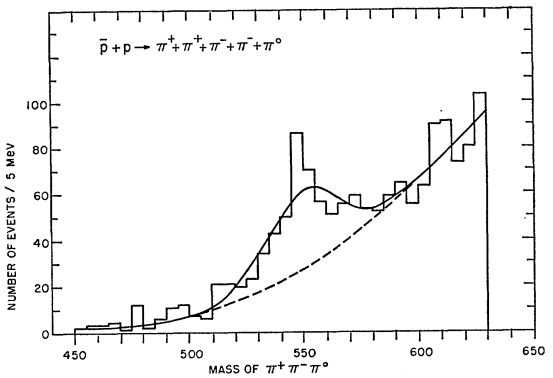

FIG. 23. Fit to the $\pi^+\pi^-\pi^0$ mass spectrum near the η^0 region in $\bar{p}+p \to \pi^+ + \pi^+ + \pi^- + \pi^- + \pi^0$.

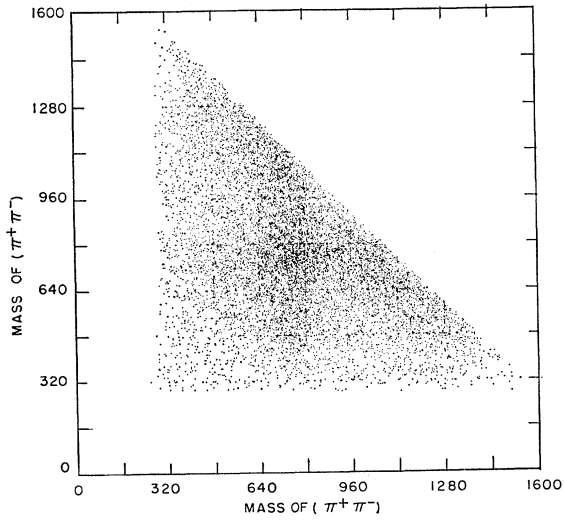

FIG. 24. Scattergram of the mass of $\pi^+\pi^-$ versus the mass of the other $\pi^+\pi^-$ in the reaction $\bar{p}+p \to \pi^+ + \pi^+ + \pi^- + \pi^- + \pi^-$. Each event contributes 4 points to the plot.

TABLE II. Parameters of the best fits used in the evaluation of ρ production rates.

Final state	Resonance	Parameters of best fit: Mass	Γ	No. of constraints	χ^2	Fraction of resonance production
$\pi^+\pi^+\pi^-\pi^-$	ρ^0	751±6	174±31	20	22.4	1.00±0.17
$\pi^+\pi^+\pi^-\pi^-\pi^0$	ρ^0	746±4	135±20	16	24.6	0.39±0.07
$\pi^+\pi^+\pi^-\pi^-\pi^0$	$\rho^+ + \rho^-$	750±3	150±30	16	14.1	0.34±0.09

to the area of the Breit-Wigner used in the best fit divided by the total number of events. These correspond to anihilation rates of $(5.8_{-1.3}^{+0.3})\%$ for $\rho^0\pi^+\pi^-$, $(7.3 \pm 1.7)\%$ for $\rho^0\pi^+\pi^-\pi^0$, and $(6.4\pm1.8)\%$ for $\rho^\pm\pi^\mp\pi^+\pi^-$.

TABLE III. Annihilation rates for channels involving the ρ, ω and η mesons.

Channel	Rate (%)
$\bar{p}+p \to \rho^0+\pi^0$	1.4 ±0.2
$\rho^\pm+\pi^\mp$	2.9 ±0.4
$\rho^0+\pi^+\pi^-$	$5.8_{-1.3}^{+0.3}$ [c]
$\rho^0+\rho^0$	0.4 ±0.3
$\rho^0+\pi^+\pi^-+\pi^0$	7.3 ±1.7
$\rho^\pm+\pi^\mp+\pi^+\pi^-$	6.4 ±1.8
$\omega^0+\pi^+\pi^-$	3.8 ±0.4 [a,c]
$\eta^0+\pi^+\pi^-$	1.2 ±0.3 [b,c]
$\omega^0\rho^0$	0.7 ±0.3
$\eta^0\rho^0$	0.22±0.17

[a] We used $(\omega^0 \to \text{all})/(\omega^0 \to \pi^+\pi^-\pi^0) = 1.14$.
[b] We used $(\eta^0 \to \text{all})/(\eta^0 \to \pi^+\pi^-\pi^0) = 3.5$.
[c] The rates quoted for the production of $\rho^0+\pi^+\pi^-$, $\omega^0+\pi^+\pi^-$, and $\eta^0+\pi^+\pi^-$ include the contributions from the events where the $\pi^+\pi^-$ were the decay products of a ρ^0 meson.

The results discussed in this section are summarized in Table III, along with some two-body rates previously published.[7] It should be pointed out that from the present analysis the possibility that the resonances in

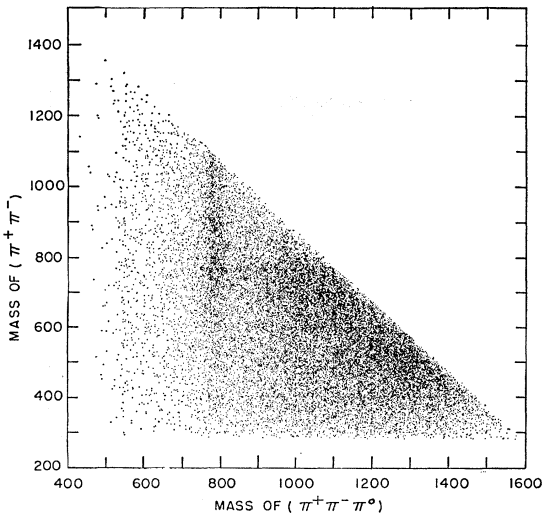

FIG. 25. Scattergra of the mmass of $\pi^+\pi^-$ versus the mass of $\pi^+\pi^-\pi^0$ in the reaction $\bar{p}+p \to \pi^+ + \pi^+ + \pi^- + \pi^- + \pi^0$. Each event contributes 4 points to the plot.

Table II are decay products of heavier resonant states cannot be excluded.

VI. $\varrho^0\varrho^0$, $\varrho^0\omega^0$, AND $\varrho^0\eta^0$ PRODUCTION

Annihilations into the two-body channels $\rho^0\rho^0$, $\rho^0\omega^0$, and $\rho^0\eta^0$ were investigated. The estimates for the annihilation rates into these channels were based on the study of two-dimensional scattergrams of invariant masses. To study $\rho^0\rho^0$ production, a scattergram was used, plotting the mass of one $\pi^+\pi^-$ combination against the mass of the other $\pi^+\pi^-$ combination in the reaction $\bar{p}+p\rightarrow\pi^++\pi^++\pi^-+\pi^-$, with each event contributing 4 points (Fig. 24). For $\rho^0\omega^0$ and $\rho^0\eta^0$ production, the mass of one $\pi^+\pi^-$ combination was plotted against the mass of the other $\pi^+\pi^-$ combined with the π^0, in the reaction $\bar{p}+p\rightarrow\pi^++\pi^++\pi^-+\pi^-+\pi^0$. Again each event contributed 4 points to the scattergram, shown in Fig. 25.

A rectangular region of the scattergram around the point which corresponds to simultaneous production of the two resonances was subdivided into nine boxes, as shown in Fig. 26. Each box has contributions from four sources: the production of resonance No. 1, the production of resonance No. 2, the simultaneous production of resonances No. 1 and No. 2, and nonresonant background with intensities α, β, γ, δ, respectively. These contributions were taken to be incoherent:

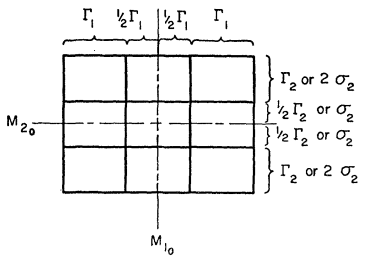

FIG. 26. Sketch illustrating the nine regions of the scatterplot of m_1 versus m_2 used to determine the rate for simultaneous production of resonances 1 and 2.

$$R1_i=\int_{m_1{}^i{}_{\min}}^{m_1{}^i{}_{\max}}\int_{m_2{}^i{}_{\min}}^{m_2{}^i{}_{\max}}\frac{\varphi dm_1dm_2}{(m_1-m_{1_0})^2+\frac{1}{4}\Gamma_1{}^2},$$

$$R2_i=\int_{m_1{}^i{}_{\min}}^{m_1{}^i{}_{\max}}\int_{m_2{}^i{}_{\min}}^{m_2{}^i{}_{\max}}\frac{\varphi dm_1dm_2}{(m_2-m_{2_0})^2+\frac{1}{4}\Gamma_2{}^2},$$

$$R12_i=\int_{m_1{}^i{}_{\min}}^{m_1{}^i{}_{\max}}\int_{m_2{}^i{}_{\min}}^{m_2{}^i{}_{\max}}\frac{\varphi dm_1dm_2}{[(m_1-m_{1_0})^2+\frac{1}{4}\Gamma_1{}^2][(m_2-m_{2_0})^2+\frac{1}{4}\Gamma_2{}^2]},$$

where

$m_1{}^i{}_{\min}$, $m_1{}^i{}_{\max}$, $m_2{}^i{}_{\min}$, and $m_2{}^i{}_{\max}$ are the boundaries of box i;

m_{1_0}, Γ_1, m_{2_0}, Γ_2 are the masses and widths of the two resonances;

$\varphi=\varphi(m_1,m_2)$ is the effective phase space.

The values of α, β, γ and δ were found by minimizing the χ^2 function

$$\chi^2=\sum_{i=1}^{9}[n_i-(\alpha R1_i+\beta R2_i+\gamma R12_i+\delta\varphi_i)]^2/n_i$$

where n_i is the observed number of events in box i.

For the case of $\rho^0\omega^0$ and $\rho^0\eta^0$, the integrals $R1$, $R2$, and $R12$ contained Gaussians instead of the Breit-Wigner forms for the ω^0 and η^0.

The results of these analyses are listed in Table III. The rate listed for $\bar{p}+p\rightarrow\rho^0+\omega^0$ is the one obtained by a different, more detailed analysis already published.[5] The rate obtained from the analysis described here was within the errors of the rate listed in Table III. The rates for $\rho^0\rho^0$ and $\rho^0\eta^0$ are not significantly different from zero.

ACKNOWLEDGMENTS

We would like to thank Professor Jack Steinberger for continuing support and interest in this work. We are grateful to the operating crews of the 30-in. hydrogen bubble chamber and the AGS staff at Brookhaven National Laboratory for their help in the exposure. It is a pleasure to acknowledge the collaboration with the Rutgers University Bubble Chamber Group in the early stages of the experiment. And finally, we thank the Nevis scanning and measuring staffs for their excellent work during the analysis.